工學碩士 學位論文

Effect of hot water environment under different bending stress on the GFRP mechanical property

指導敎授 金 允 海

2015年 08月

韓國海洋大學校 大學院

材 料 工 學 科

胡 伟 光

本 論文을 胡伟光의 工學碩士 學位 論文
으로 認准함.

위원장　　文 慶 萬　　　（인）

위　원　　河 鎭 喆　　　（인）

위　원　　金 允 海　　　（인）

2015年 07月

韓國海洋大學校 大學院

Contents

List of Tables

List of Figures

Effect of hot water environment under different bending stress on the GFRP mechanical property

Hu, Weiguang

Department of Materials Science and Engineering
Graduate School of Korea Maritime and Ocean University

Abstract

The mechanical properties of composites are greatly affected by the environment. In this research, the glass fiber unsaturated polyester composite materials (GFRP) under different bending stress and submerged in hot water at a temperature of 80℃ is investigated. Loading 100 H (hours), 200 H, 400 H, 600 H, 800 H for testing under stresses equal to 0% (zero pressure), 30%, 50% and 70% of the material ultimate strength are applied on samples. Then water absorption ratio is analyzed, and by experiment data of bending stress and modulus of elasticity in bending after three-point bending test, failure time, life curve, normalized strength degradation model and the fracture energy of composites are analyzed. Finally the change of material interface affected by the environment is observed with optical microscope and SEM, and the reasons of the change of material mechanics properties are explained.

KEY WORDS: GFRP; Three-point bending test; Water sorption; Life curve; Fracture energy

Chapter 1 Introduction

1.1 General background

Material is not only the material basis of human existence, but also an important indicator of social development. In recent years, with its rapid development of excellent performance, composite materials are more and more widely used in our lives. Fiberglass as an important part of composite materials, which is commonly known today, was invented in 1938 by Russell Games Slayter of Owens-Corning as a material to be used as insulation. It is marketed under the trade name Fiberglas, which has become a genericized trademark. Although the intensity is high for fibers, but it can only sustain tension because of the soft body, and it is difficult to bear bending, shear and compressive stress, also not easy to make a fixed geometry. It can be made all kinds of solid products with fixed shape, and withstood tensile stress, bending, compression and shear stress if use synthetic resin put them together. When glass fiber is used as a reinforcing agent for many polymer products; to form a very strong and light fiber-reinforced polymer (FRP) composite material called glass-reinforced plastic (GFRP), popularly known as "fiberglass"[1]. GFRP have been widely used for structural materials in water environments such as fishing trawlers, ships, reservoirs, under sea pipes, because of its good water resistance and corrosion resistance, high strength, high elastic modulus and light-weight [2, 3]. Fig. 1 shows the application of GFRP in our lives.

Dragon boat   Fluid reservoir

Fig. 1   The application of GFRP in our lives

1.2 Main research significance

Actually, the mechanical properties of GFRP are always affected by environmental factors such as temperature, humidity, ultraviolet radiation environment, etc., and it decrease badly. The phenomenon is known as aging. GFRP products will be subjected with all kinds of stress from different directions and different sizes in practical application, and it will be great influence on the service life of GFRP. GFRP product failure could cause serious economic losses and even life-threatening, so it is necessary to study the change rule of mechanical properties when GFRP under different environments. In general terms, decrease of mechanical properties is mainly caused by varying degrees of damage to the resin matrix, the fibers reinforced and resin / fiber bonding interface [4]. A number of studies have been carried out to study the aging of composite material. Such as Lv Xiaojun, Zhang Qi, Ma Zhaoqing, et al. In their research, the mechanical properties of carbon fiber / epoxy resin composites were studied at the temperature of 30℃ and 80℃, and performance of composites was decreased obviously at 80℃[5]. A.Nakai,S. Ikegaki and H. Hamada researched the Degradation of braided

composites in hot water at a temperature of 80℃[6]. The effects of soaking time on the mechanical properties of water are also important. As the aging time increases, the mechanical properties of the materials will be decreased. Sun Bo, Li Yan's research shows that glass fiber epoxy resin in different temperatures of water aging, mechanical properties decreased significantly in the first 8 weeks. The rate of decline in the first 4 weeks is fast, and a year later tends to be stable[7].

In this research, the glass fiber unsaturated polyester composite materials（GFRP） submerged in hot water at a temperature of 80℃ by the time of 100 H (hours), 200 H, 400 H, 600 H, 800 H. The specimen were under stresses equal to 0%（zero pressure）, 30%, 50% and 70% of the material ultimate strength and the change rule of material mechanical properties was studied.
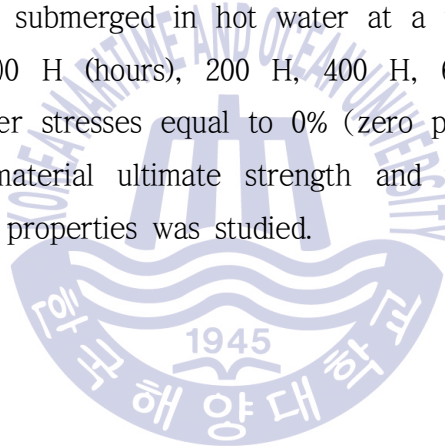
Chapter 2 Experiment

There are many kinds of methods to produce the GFRP, such as the hand lay-up method, reaction injection molding method, RTM (resin transfer molding) method and VARTM (vacuum-assisted resin transfer molding) method, etc. In this study, VARTM method technology are used for making glass fiber unsaturated polyester composites, and the specimen are cut according to ASTM D790-2010 standard. Specimens are pressed on bending stress equal to 0%, 30%, 50%, 70% of the material ultimate strength by pressure fixture and placed in the water environment at 80℃ for 100 H, 200 H, 400 H, 600 H, 800 H. Then water absorption ratio is analyzed, and by experiment data of bending strength and modulus of elasticity in bending after three-point bending test, failure time, life curve, normalized strength degradation model and the fracture energy of composites are analyzed. Finally the change of material interface is affected by the environment is observed with optical microscope and SEM.

2.1 Experimental material

Glass fiber cloth article number∶#KN 2100-N2. The information of glass fiber cloth shows in Table 1, and the glass fiber cloth shows in Fig. 2.

Unsaturated polyester: EPOVIA®LSP-8020B. The unsaturated polyester shows in Fig. 3.

Hardener: Butanox M-60. The hardener shows in Fig. 4.

The proportion of resin and hardener: 100:1; The GFRP is made at normal pressure and temperature

Collection
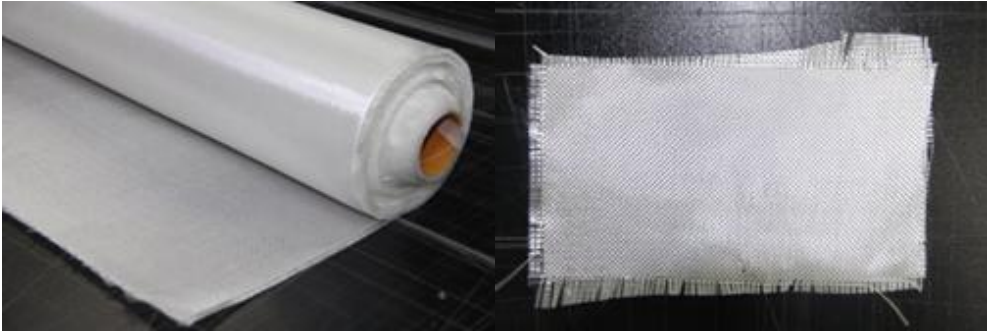
Fig. 2 Glass fiber cloth

Fig. 3 Unsaturated polyester

Fig. 4 Hardener

Table 1 Glass fiber cloth

Item		Glass fiber cloth
Item number		#KN 2100-N2
Fibrous tissue		Plain weave
Glass fiber	Warp	ECG 37 1/10(135tex)
	Weft	ECG 37 1/10(135tex)
Density (dtex / 25 mm)	Warp	18
	Weft	18
Tensile strength (kg/25mm)	Warp	90(above)
	Weft	90(above)
Width (mm)+15		1,020
Thickness(mm)+0.08		0.21
Weight(g/m2)+5%		190
Surface treatment		F.R.P resin
Package unit		200M/ bundle

Glass fiber continuous filament yarn
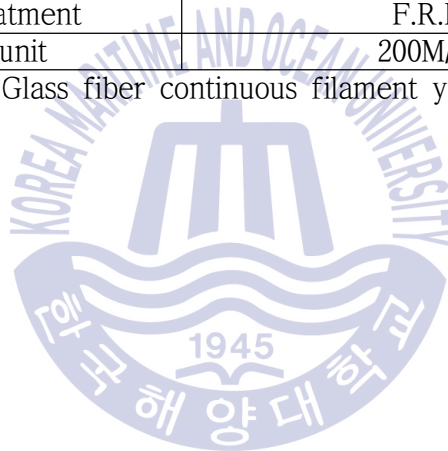
2.2 VARTM method technology

In the VARTM process, the mold release agent is coated with a one-sided mold firstly, the tailored glass fiber is placed in mold neatly, and the plastic tube is fixed on both ends of fibers. Put the mold release membrane, isolation cloth and flow medium over the fiber, and a vacuum bag is placed over the top to form a vacuum-tight seal. Then vacuumize the system by vacuum pump, and the unsaturated polyester and hardener mixture are entered in the structure by plastic tube from side to the other side slowly. Finally, seal both ends when the mixture is filled with the system. Experimental stages are shown in Fig. 5 and Fig 6. The production, which is manufacturing by VARTM, is low cost, low void content, less toxic vapors produced during molding, high product performance and flexibility of large molding process [8].
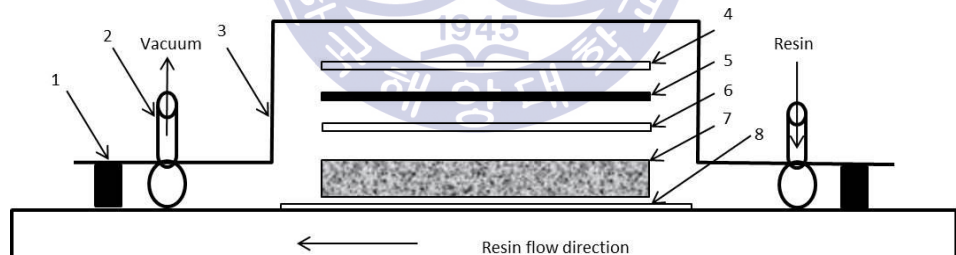
1. Sealing tape   2. Plastic tube   3. Vacuum bag   4. Flow medium
5. Isolation cloth   6. Mold release membrane   7. Fiber   8. Mold release

Fig. 5 VARTM method technology

Fig. 6 Process of manufacturing specimens

2.3 Composite materials cutting

Cut the specimen according to ASTM D790-2010 standard with the cutting machine shown in Fig. 7. Detailed parameters of specimen and experimental conditions are shown in Table 2. The specimen is shown in Fig. 8 and the quantities of specimens are shown in Table 3.

Fig. 7 Cutting machine

Fig. 8 Specimen

Table 2 Detailed parameters of specimen and experimental conditions [9]

Specimen	GFRP			
Stacking direction	[0° ,90°]			
Specification	ASTM D790-2010			
Temperature	Room temperature, dry			
Test speed	5.46mm/min			
Unit : mm	T	W	LO	L
Dimension(ASTM)	3.2	25	140	102.4

Table 3 Quantities of specimens (piece)

Time Stress	0 H	100 H	200 H	400 H	600 H	800 H
0%	6	6	6	6	6	6
30%		6	6	6	6	6
50%		6	6	6	6	6
70%		6	6	6	6	6

2.4 Bending stress

The material ultimate strength of the bending stress can be got by three-point bending test, and corresponding ultimate displacement is obtained at the same time. In this way, the bending stress procedure is controlled by displacement. In this research, constant pressure is pressed to specimen by pressure fixture shown in Fig. 9. 0%, 30%, 50%, 70% of the material ultimate strength is pressed to specimen by pressure fixture with different displacement.
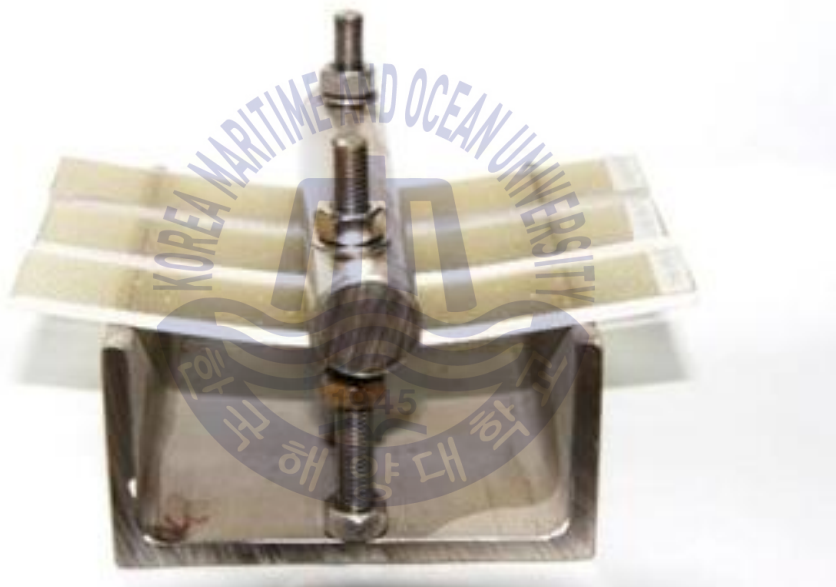
Fig. 9 Pressure fixture

2.5 Water environment at a temperature of 80℃

Specimens are applied constant pressure and put into the water tank which the temperature can be controlled at $80\pm1℃$ for 100 H, 200 H, 400 H, 600 H, 800 H. The water tank is shown in Fig. 10.

Fig. 10 Water tank

2.6 Three-point bending test

Then remove the specimen, after dry and weigh them, analyze the impact of the conditions to mechanical properties of materials by three-point bending test by universal testing machine (UTM). The experimental process is shown in Fig. 11. Calculate the rate of crosshead motion as follows and set the machine for the rate of crosshead motion as calculated by Equation 1:

$$R = ZL^2/6d. \tag{1}$$

Where R is rate of crosshead motion, mm (in.)/min, L is support span, mm (in.), d is depth of beam, mm (in.), and Z is rate of straining of the outer fiber, mm/mm/min (in./in./min). Z shall be equal to 0.01. In no case shall the actual crosshead rate differ from that calculated using Equation 1, by more than ± 10 % [10].
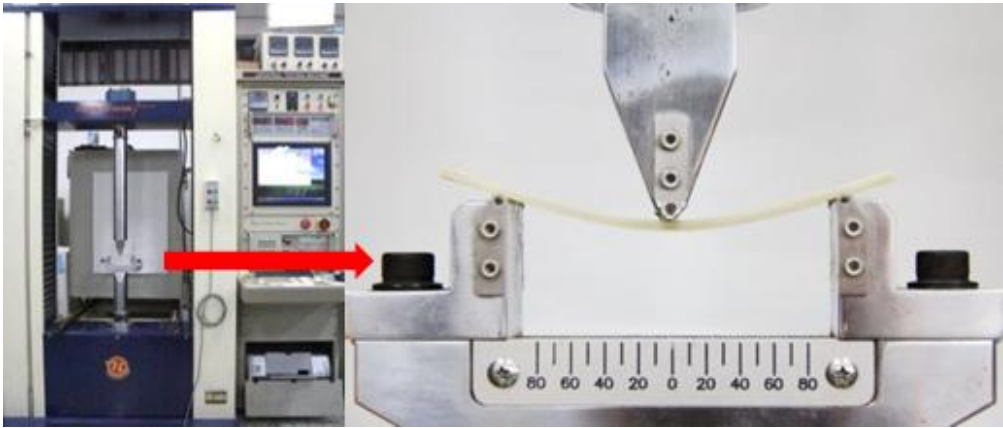
Fig. 11 Three-point bending test

Chapter 3 Analysis and results

3.1 Water absorption rate

Liquid molecules often diffuse into solid materials and it is present in the materials in the form of physical or chemical. The rate of water absorption is depended on both the solid and the liquid. The water absorption ratio of the composite panel W (%) can be calculated by the simple expression [11, 12, 13]:

$$W = \frac{W_t - W_0}{W_0} \times 100\%.$$ (2)

Where W_t is the mass of the panel after a given immersion time and W_0 is the original panel mass.

Fick's laws of diffusion describe diffusion and were derived by Adolf Fick in 1855. They can be used to solve for the diffusion coefficient. Fick's first law relates the diffusive flux to the concentration under the assumption of steady state. In one (spatial) dimension, the law is:

$$F = -D\frac{\partial C}{\partial Z}.$$ (3)

Where F is the diffusion flux, D is the diffusion coefficient, C is the concentration of diffusion material, Z is the position.

$$\frac{\partial C_{(Z,t)}}{\partial t} = D\frac{\partial^2 C_{(Z,t)}}{\partial^2 Z}.$$ (4)

Where C is the concentration in dimensions of length, t is the time, D is the diffusion coefficient in dimensions of length, Z is the position of length [14].

For water to the plate plane (perpendicular to the plate surface) one-dimensional diffusion, boundary conditions:

$$C_{(Z,0)} = C_0. \tag{5}$$

$$C_{(-h/2,t)} = C_{(h/2,t)} = C_\infty \, t > 0. \tag{6}$$

Where, C_0 is the initial concentration of water in the material; C_∞ is the equilibrium moisture concentration; h is the plate thickness. Through the Equation (4), obtaining the equation:

$$\frac{C - C_{(0)}}{C_\infty - C_{(0)}} = 1 - \frac{4}{\pi} \sum_{n=0}^{\infty} (2n+1)^{-1} \sin\left[\frac{(2n+1)Z\pi}{h}\right] \exp\left[-\frac{D(2n+1)^2\pi^2 t}{h^2}\right]. \tag{7}$$

Compute the integral for Z from $-h/2$ to $h/2$, and set $M_t = \int_{-h/2}^{h/2} C(x,t)dx$, obtaining:

$$\frac{M_t - M_{(0)}}{M_\infty - M_{(0)}} = 1 - \frac{8}{\pi^2} \sum_{n=0}^{\infty} \frac{1}{(2n+1)^2} exp[-D(2n+1)^2\pi^2 t/h^2] \tag{8}$$

$M_0 = \int_{-h/2}^{h/2} C(x,t_0)dt$; $M_\infty = \int_{-h/2}^{h/2} C(x,t_\infty)dt$; M_t in the Equation (8) is the water absorption ratio at time t, and M_∞ is the maximum water absorption ratio, D is the diffusion coefficient in dimensions of length, h is the position of length. While $M_0=0$, the Equation (8) changes to:

$$\frac{M_t}{M_\infty} = 1 - \frac{8}{\pi^2} \sum_{n=0}^{\infty} \frac{1}{(2n+1)^2} exp[-D(2n+1)^2\pi^2 t/h^2] \tag{9}$$

When t is not big, the summation on the right side is accurately enough to just take one term (n = 0), so the Equation (9) can be

– 14 –

written as:

$$\frac{M_t}{M_\infty} = 1 - \frac{8}{\pi^2} exp[-D\pi^2 t/h^2].\tag{10}$$

  Fick moisture model can describe the composite hygroscopic law well. At the beginning, materials absorb water fast, the water absorption rate is nearly constant; after a certain time, the water absorption rate gradually slow down, and finally close to zero, entering a relative saturation stage. It is basic characteristics of obey Fick's law curve [15, 16]. Fig. 12 shows the water absorption rate of the specimen change with time under different bending stress. Bending stress has no effect for water absorption rate, and it obey Fick's law curve well in 800 H. This stage is mainly due to the composite material itself defects, cracks and moisture absorption of the resin itself, under the combined effect of temperature and humidity, the water quickly through the voids and cracks into the interior material.
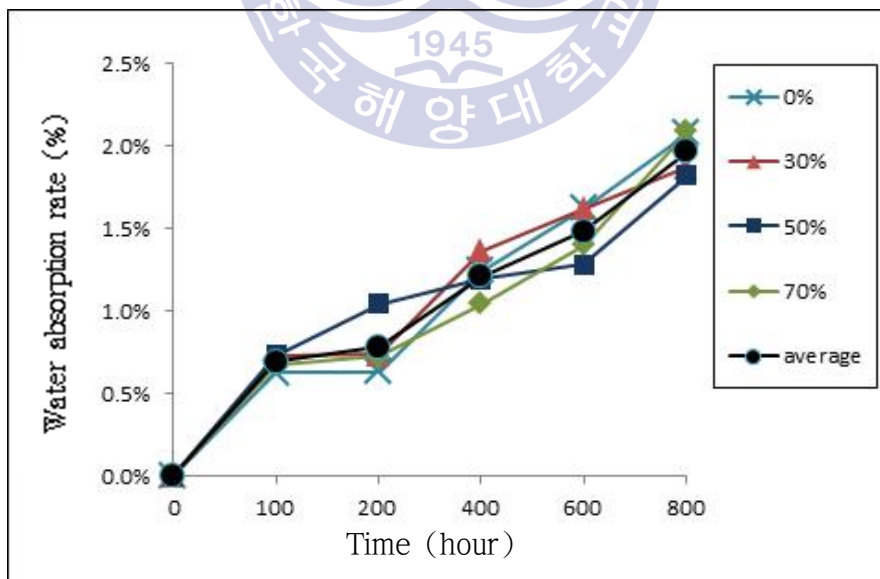
Fig. 12 The water absorption rate change with time under
different bending stress
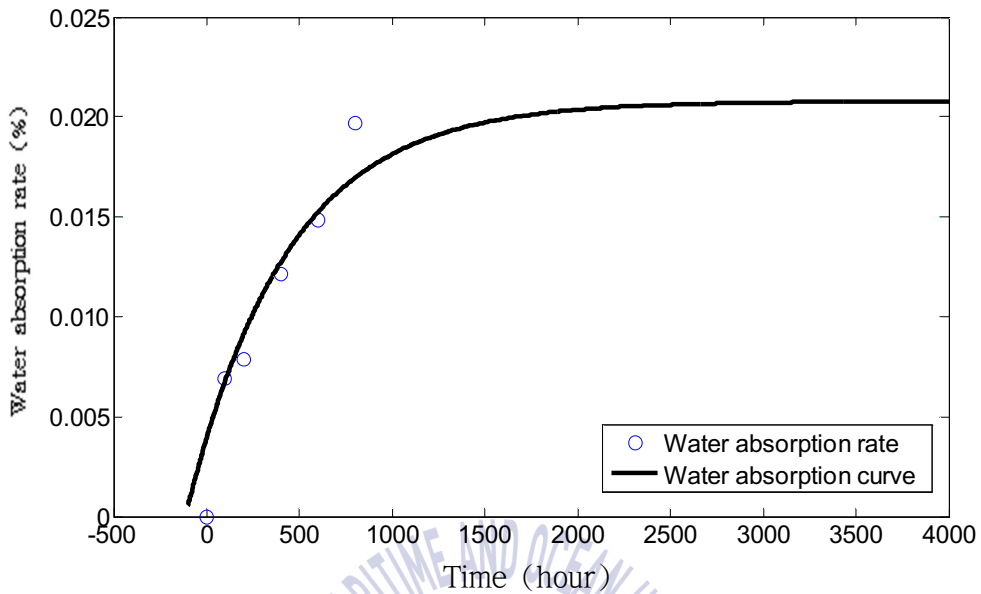
Fig. 13 The tendency of the water absorption rate at 80℃

When the experimental result is substituted into Equation (10), M_∞ and D of materials in hot water at 80℃ are solved by Matlab software. The result shows in Table 4. The tendency of the moisture absorption rate is shown in Fig. 13. The moisture absorption rate of material is symmetrically before 1000 H, then the curve gradient significantly smaller than before. Due to its water absorption process is more complicated, the resin may have chemical changes after absorbent the water a long time.

Table 4 The value of M_∞ and D

constant	M_∞	D
value	0.02077	0.001917

3.2 Bending modulus of elasticity

Modulus of Elasticity is the ratio, within the elastic limit, of stress to corresponding strain. It is calculated by drawing a tangent to the steepest initial straight-line portion of the load-deflection curve and using Equation (14):

$$E_B = L^3 m / 4bd^3. \tag{11}$$

Where E_B is modulus of elasticity in bending, MPa(psi), L is support span, mm(in.), b is width of beam tested, mm(in.), d is depth of beam tested, mm(in.), and m is slope of the tangent to the initial straight-line portion of the load-deflection curve, N/mm (l bf/in.) of deflection [10].

Each dot represents the modulus of elasticity in bending under different bending stress in different time is shown in Fig. 14. The modulus of elasticity in bending is decreased firstly, then it is increased with the increasing immersion time, finally it has a downward trend. The degree of decrease of the flexural modulus decreases with increasing pressure. And the recovery of flexural modulus is influenced by pressure. It recovers fast when the pressure is low, and recovers slow when the pressure is high.
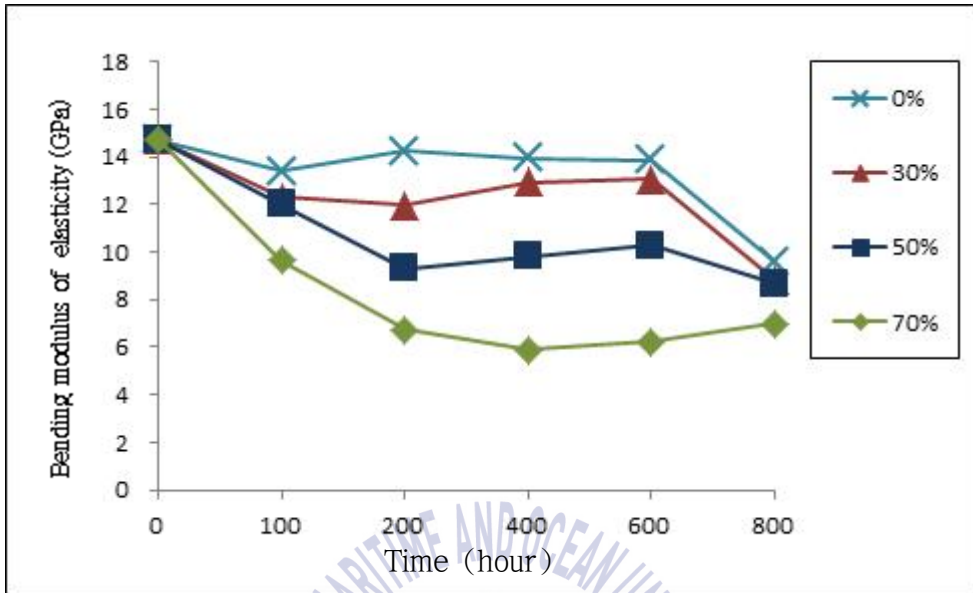
Fig. 14 The change of modulus of elasticity in bending with
time under different bending stress

3.3 Bending Strength

When a homogeneous elastic material is tested in flexure as a simple
beam supported at two points and loaded at the midpoint, the maximum
stress in the outer surface of the test specimen occurs at the midpoint.
This stress may be calculated for any point on the load-deflection curve
by means of the following equation:

$$\delta_f = \frac{3PL}{2bd^2}. \tag{12}$$

Where δ_f is stress in the outer fibers at midpoint, MPa(psi), P is load
at a given point on the load-deflection curve, N (lbf), L is support
span, mm (in.), b is width of beam tested, mm (in.), and d is depth of
beam tested, mm (in.) [10].

Each dot in Fig. 15 shows the residual bending strength of material under different pressure with time. The distribution of the dots in the figure shows the residual bending strength of the material is reduced with the increase of time, and it decreases fast as the pressure increases. When pressure is applied, the residual bending strength of the material decreases rapidly within the first 100 H, and it decreases slowly from 100 H to 800 H, it declines faster when pressure increases. The change of decreasing rate of bending strength with pressure and time shown in Fig. 16 and the relationship between decreasing rate of the residual bending strength and the rate of pressure increase in 100 H shown in Fig. 17. Thus, in 100 H, the rate of decrease of the residual bending strength is in direct proportion to the rate of pressure increase, the fitting function is y = 0.6179x + 0.0803; where y is the rate of decrease of the residual bending strength and where x is the rate of pressure increase. The rate of decrease of the residual bending strength is low from 100 H to 800 H, and it has not connection with pressure, almost all below 10%. The sample degradation strength is fitted an exponential function form $y = ae^{bx} + ce^{dx}$ is presented. Mechanical property degradation of composites has an exponential slump by considering the physics of the problem. In Table 5, a, b, c, and d constants and statistical values for residual bending strength degradation curves are shown. Also, strength degradation curves for four states of stress are shown in Fig. 18 [17].
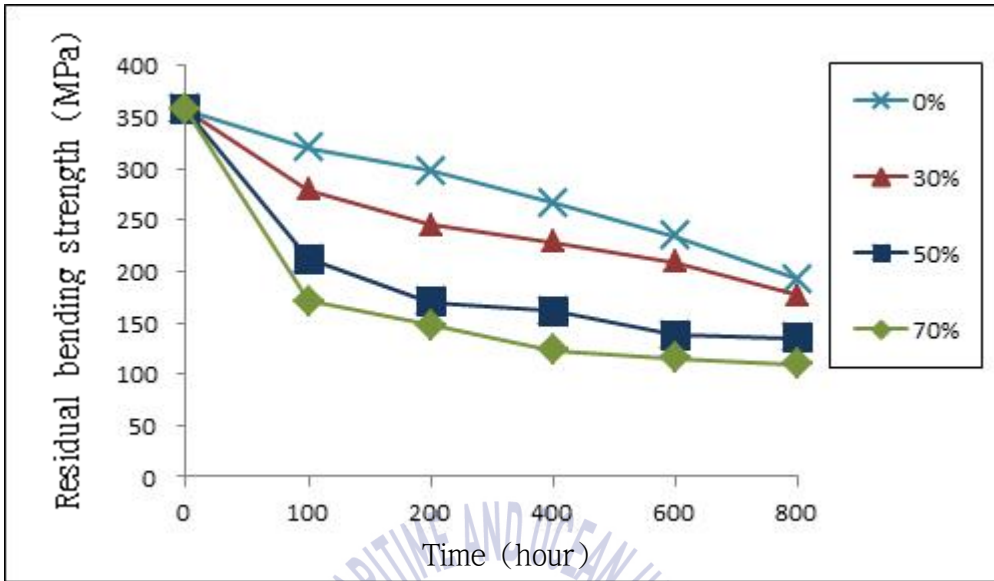
Fig. 15 The residual bending strength under different
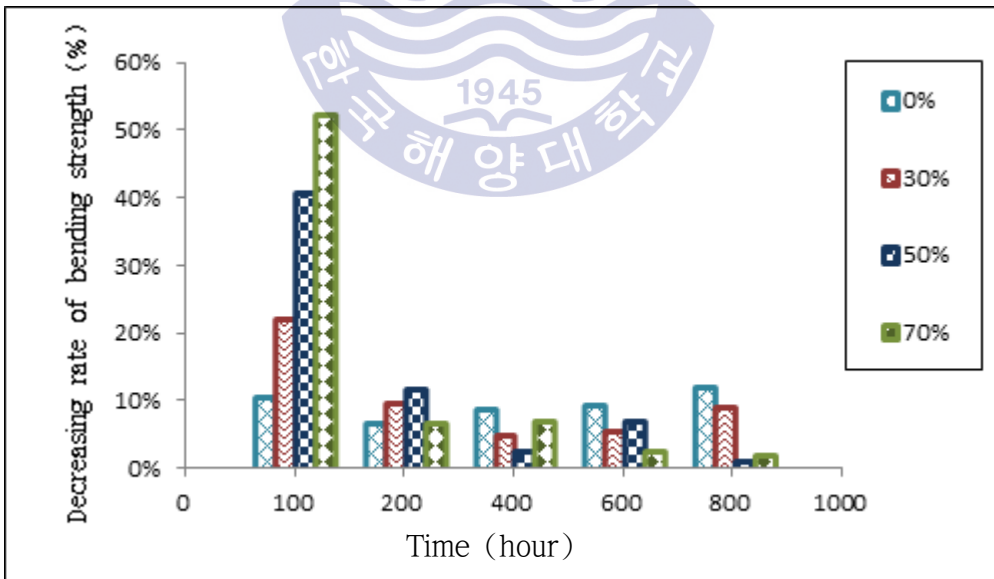bending stress with time

Fig. 16 The change of decreasing rate of bending strength
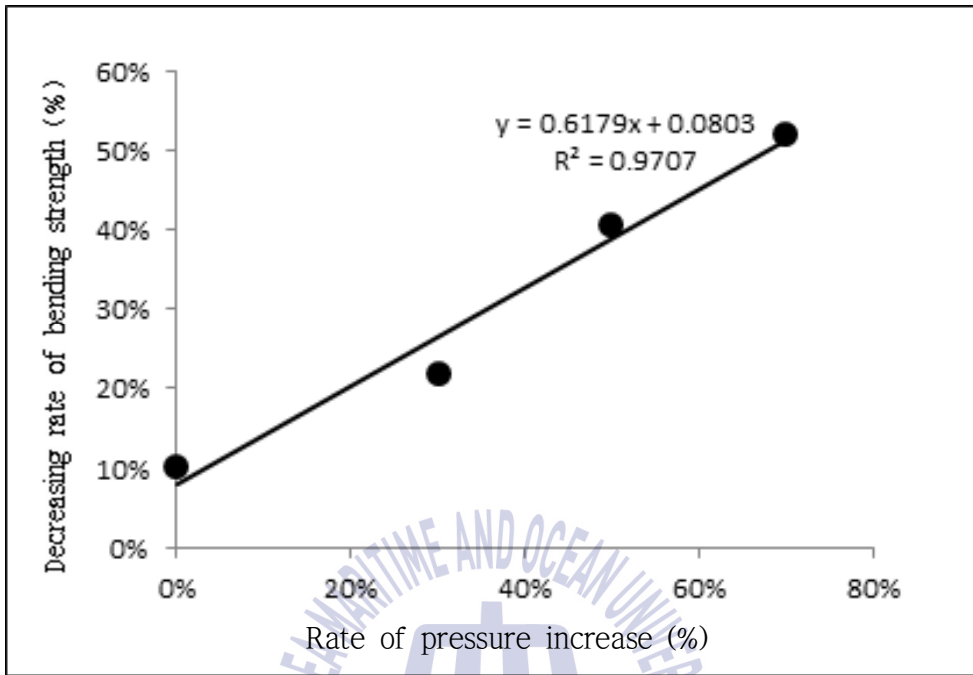under different states of stress with time

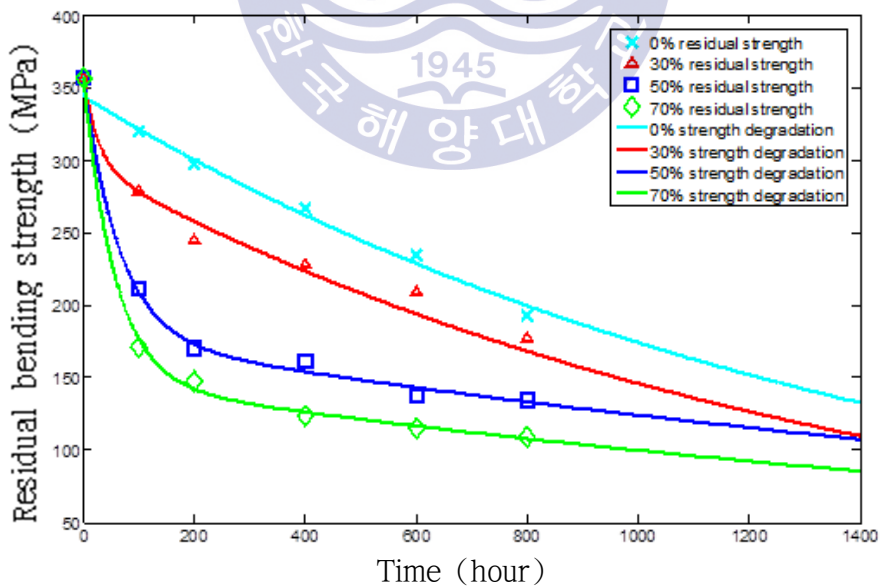Fig. 17 The relationship between decreasing rate of the residual

Fig. 18 Residual bending strength degradation curves under
different states of stress whit time

Table 5 a, b, c, and d constants and statistical values for residual bending strength degradation curves

Curve	a	b	c	d	R-Square
0%	12.66	−1.643	344.1	−0.0006808	0.9935
30%	59.6	−0.03735	297.1	−0.0007107	0.9783
50%	179.6	−0.01558	177.4	−0.00035757	0.9967
70%	210.3	−0.01788	147.3	−0.0003889	0.9982

The mechanical properties of composite materials will be affected after absorbing water, and the change is quite different with the bending stress. Hence, the bending stress must be considered at the same time. In order to know the reasons of the decrease of mechanical properties, consider the influence of each component of composite materials in the hot water environment is necessary.

The influence of moisture on resin matrix is water swelling in the matrix. The tensile stress is produced between the interface of fiber and matrix along the direction of fiber radial, and it accelerate the absorption of water. Swelling makes matrix macromolecular structure spacing increases, the stiffness group activity increases, thus make the matrix plasticizing, the result is the glass transition temperature of the composite material after moisture absorption decline and the impact toughness increased. The osmotic pressure makes the internal matrix produce tiny cracks or other types of shape change during water molecules diffusing. Water contributes to the spread of the crack, can make the matrix burst, and substrate hydrolysis leads to chain scission reconciliation crosslinking. Matrix swelling and plasticizing are reversible, called physical aging, at this point, the chemical structure is not affected, and material resumed after drying, but the performance

changes significantly related with the temperature. Matrix crack spread and hydrolysis are irreversible, the damage to the material is permanent.

Water resistance of fiber is one of the influencing factors of composite water resistance. For all kinds of reinforcing fiber, carbon fiber has better moisture resistance than glass fiber, and aramid fiber is worst of the three. The performance of axial change is usually available to characterize the effect of fiber in the composite material under hot and humid environment. Studies have shown that hygroscopic nearly does not affect the tensile properties of the unidirectional composite material.

The good mechanical properties cannot be assured without good interface bonding for fiber and resin. But erosion of interface will happen after composite material absorb moisture. And the erosion degree has a great relationship of humidity, temperature, as well as the handling of the fiber surface. It can produce a shear stress of the fibers because of matrix swelling. The interfacial bond will be destroyed when the shear stress is greater than the adhesion stress of interfacial bond, and thus stresses cannot transfer effectively. Water molecules penetrate into the interior of the material system gradually to reduce the force between macromolecules, further accumulation of water molecules form blisters. Due to the penetration of water molecules lead to the matrix resin molecular chain rupture, chemical degradation occur, molecular weight decrease, interface crack grow, the chemical combination of fiber and matrix destroyed. The destruction of the interface is irreversible damage, and the impact on the material is permanent. Due to the capillary effect of acceleration, interface diffusion is the important reason for the composite wet and heat aging.

The main mechanism of temperature on the thermal expansion coefficient of the fiber and the matrix do not match. It causes the residual stress, which leads to micro-cracks increased, broad interface degumming, and the fracture toughness of the laminate reducing. Furthermore, thermal stress caused by high temperature, result in more delamination area and long fibers pulled out, and when the temperature exceeds the glass transition temperature, the plastic substrate increases, the ability of the laminate to improve resistance to delamination.

In this experiment, after the GFRP absorbed water, due to the resin swelling can cause swelling stress, which can counteract the effect of the curing residual stresses, so that properties of the composites increased; in addition, resin secondary curing reaction may occur in GFRP because of the resin is not sufficiently cured before at high temperature, it will help to improve the material properties. However, fiber will withstand shear stress after resin absorbed water, when the stress reaches a certain magnitude than the fiber / matrix interfacial bond strength, The result is interfacial debonding, lower transmission capacity to carry the interface, and the moisture leads to matrix macromolecules plasticized, increases the distance between the molecular chains, can destroy intermolecular van der Waals force. Further, after the moisture diffusion into the resin matrix, the matrix may occur with certain polar groups of chemical reaction, resulting in the hydrolysis of the substrate, or chain scission, weaken chemical bonding between molecules. Due to various factors, the mechanical properties of GFRP change up-and-down with the increase of time, but overall Modulus of elasticity show a downward trend [15, 17]. There is a stress of the separated between layer and layer within the material with a long time bending stress, which make material stratification easier. So with the

increase of the bending stress, the reduction of material mechanical properties is more obviously.

3.4 Extrapolation of time to failure (TF)

Time to failure (TF) is the time when the residual strength of samples reaches to the magnitude of applied stress. For example in 30% stress state, TF is the time when the magnitude of the residual strength of the sample is equal to 30% of the material ultimate strength. It's impossible to measurement of TF directly in displacement control test. So, samples are submerged in hot water at a temperature of 80℃ for a specific time and removed from the water. Then the residual bending strength of the sample is measured by three-point bending test. Using cubic spline method and extrapolation of the data, time to failure under different state of stress is calculated. The results are summarized in Table 6 [17].

Table 6 TF values in different stress states

The stress state	0	30%	50%	70%
Residual strength （MPa）	356.725	107.018	178.363	249.708
Time to failure （h）		1223.3	163.5	40.8

3.5 Life curve (S-T)

Due to S-T curve also fit an exponential function $y=ae^{bx}+ce^{dx}$, using TF values in Table 6, TF points for the samples under bending stress equal to 30%, 50% and 70% of the material ultimate strength states and static strength of the material, S-T curve is derived and shown in Fig. 19 with strength degradation curves for three states of stress. In Table 7, a, b, c, and d constants and statistical values for S-T curves are shown [14].
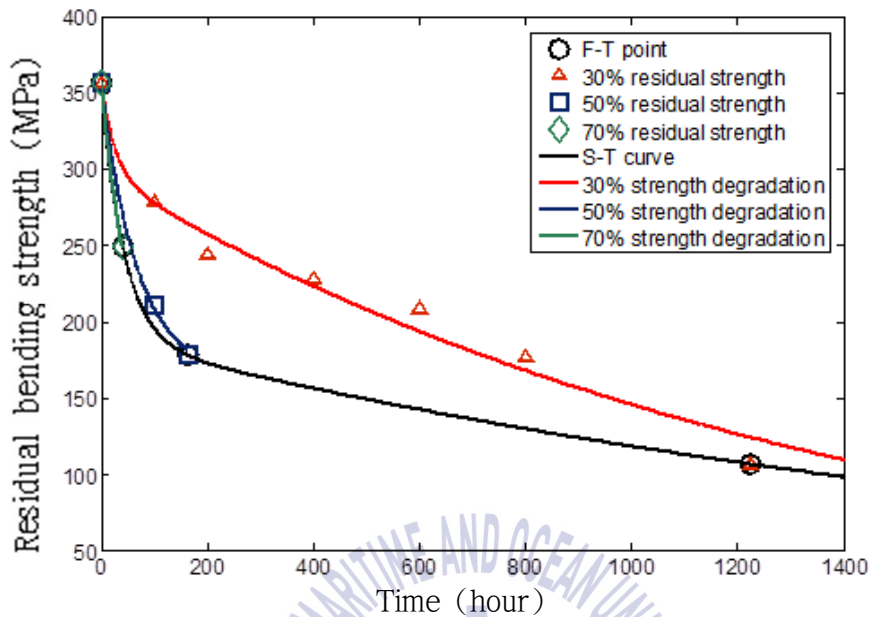
－ 25 －

Fig. 19 Strength degradation curves for different stress states and S-T curve

Table 7 a, b, c, and d constants and statistical values for S-T curves

Curve	a	b	c	d	R-Square
S-T	168.3	-0.02339	188.4	-0.0004623	1

3.6 Normalized strength degradation model

All data points for the three states of stresses can be collapsed to a single curve by using the normalization technique. The Equation (13) is developed for strength degradation of a unidirectional ply under fatigue loading condition:

$$R(n,\sigma) = [1 - (\frac{\log(n) - \log(0.25)}{\log(N_F) - \log(0.25)})^r]^{1/\alpha}(R_S - \sigma) + \sigma \qquad (13)$$

Where R (n, σ) is residual strength as a function of number of cycles (n) and stress state (σ), n is number of cycles, σ is state of stress, N_F is number of cycles to failure, α and γ are independent experimental parameters, R_S is static strength [19]. Physics of the problem in fatigue behavior of composites is very similar to stress corrosion cracking of composites. As it is seen from previous decades in different research, stress corrosion cracking phenomenon is named as static fatigue. The similarity of these phenomena can be shown by replacing n parameter (number of stress cycles) with t parameter (stress corrosion exerting time). This type of modeling has been performed in a research presented by Lavoir et al. [17].

In this research, some parameters should be replaced. To replace n with t (stress corrosion exerting time), NF with TF (stress corrosion time to failure), and log0.25 should be omitted, because of non-existence of such a term in this experiment phenomenon in Equation (13), the following equation is derived.

$$R(t,\sigma) = [1 - (\frac{\log(t)}{\log(T_F)})^\gamma]^{1/\alpha}(R_S - \sigma) + \sigma \; . \tag{14}$$

Using Equation (14) and the results of tests, an equation with a form of is fitted to the points. The magnitudes of α and γ are calculated by Matlab software. These magnitudes are summarized in Table 8. Using the present model, residual strength of the composite material under hot water in different stress states and arbitrary time is predictable. In Fig. 20 the normalized bending strength degradation curve is shown [17].

Table 8 Constants and statistical values for normalized bending strength degradation curve

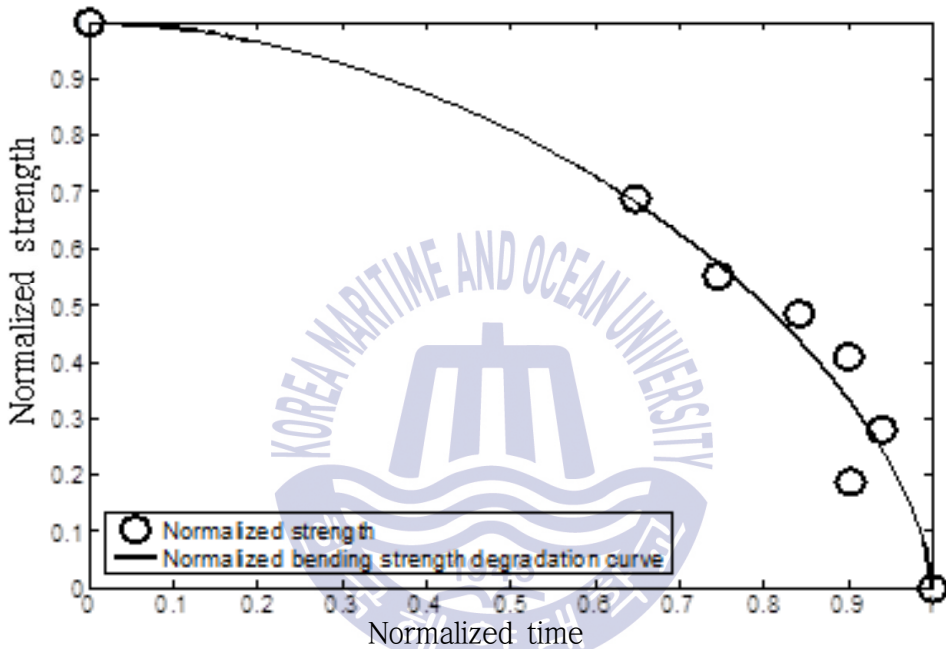| Constants	α	γ	R-Square
values	1.608	1.788	0.9564

Fig. 20 Normalized bending strength degradation curve

3.7 Fracture energy

According to the fictitious crack model, the fracture energy is the energy required to produce a unit area of crack (full broken). The model contains an assumption that is there is no energy consumption outside of the cohesive force distribution area. It means specimen fracture energy completely provided by the external force. If a specimen

is statically fractured and the work (W_F) applied to fracture the interface is measured, the approximate interface fracture energy (G_F) can be computed as:

$$G_F = \frac{W_F}{A} = \frac{\int P d\delta}{A}.$$ (15)

Where A is the area of specimen fracture section, P is the external force, δ is the displacement [20, 21]. Each point represents the fracture energy under different bending stress in different time is shown in Fig. 21. The figure shows that the fracture energy decreases with increasing immersion time and pressure, and the change is similar to bending stress, it decreases quickly before 100 H, the fracture energy attenuation for exponential function $y = ae^{bx} + ce^{dx}$, curve fitting is shown in the Fig. 21, all constants and statistical values are solved by Matlab software and shown in Table 9.

Table 9 Constants and statistical values for fracture energy degradation curve

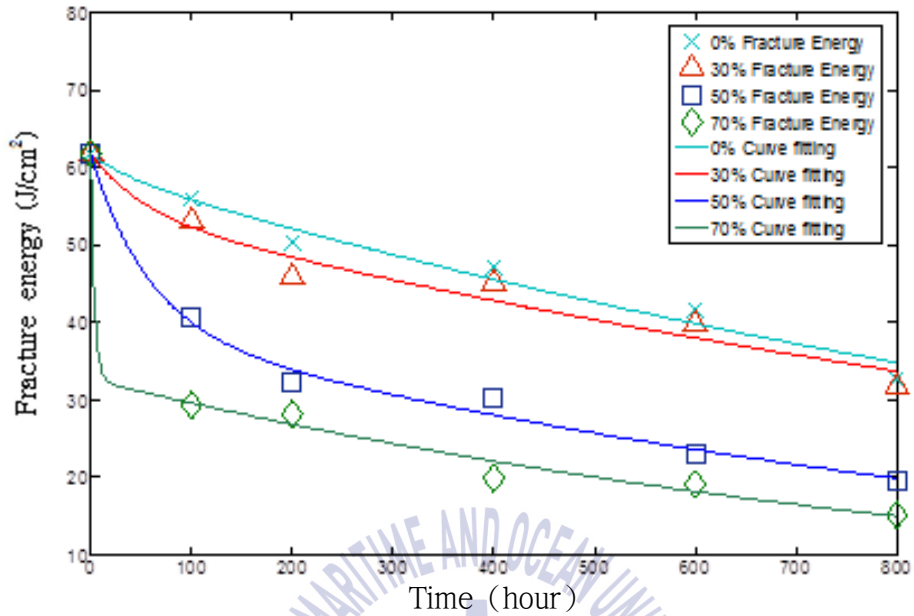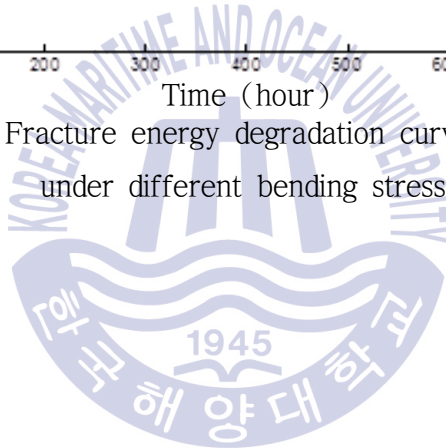| Curve	a	b	c	d	R-Square
0%	2.168	−0.02787	59.58	−0.000672	0.9745
30%	7.42	−0.01912	54.37	−0.0005961	0.9637
50%	22.23	−0.01781	39.55	−0.000859	0.9926
70%	29.11	−0.263	32.63	−0.0009715	0.9947

Fig. 21 Fracture energy degradation curve whit time
under different bending stress

Chapter 4 Optical microscope and SEM observation

Generally, specimen fracture can be divided into three parts by the three-point bending: by loading the top side of the column section is loaded indenter indentation; the middle part of the sample is compressed area; lowermost part of the specimen tensile fracture zone. Fig. 22 successively shows the specimen fracture after the three-point bending experiment without submerged in hot water (0 H) and submerged in hot water 100 hours (100 H) and 800 hours (800 H) at a temperature of 80℃. Through Fig. 23, it can be observed that specimen tensile area is much more serious damage than pressure area. Tensile fracture area, there are very obvious cracks between layers, and on the (0, 90) ply has a very significant main crack along the vertical development, and the crack through between the layers. In Fig. 22 we can see specimen without submerged in hot water is primrose yellow and transparent. 100 H test later, the specimen becomes non-transparent because of water intrusion. And 800 H later, the specimen is no longer transparent by reason of the action of water on the specimen is more serious. After bending experiment to specimen 0 H, in addition to fracture cracks, there is a long trace of glass fiber and resin debonding at both sides of the fracture cracks. The reason is the area affected a lot of tension so that glass fiber and resin debonding is happened. It also shows that the combination of glass fiber and resin are very strong and resin has played a very good stress transfer effect. This phenomenon also be

found on the specimen 100 H, but the debonding area is shorter relative to specimen 0 H, and it could not be found on specimen 800 H . The above phenomena explain one of important reasons for materials mechanical properties reduce under bending stress in the hot water environment is with the effect of water molecules, fiber and resin separation become more easily, and transfer stress become weakly.

Fig. 22 Three-point bending experiment specimens

Fig. 23 shows the surface of three-point bending experiment specimens. With the increase time, fiber and resin bonding is more and more weak, and it became layered obviously. There is subtle difference between the content of fiber and resin can be observed at the surface. The more resin pieces can be observed at the surface of spacemen 0 H than 100 H and 800 H. Fig. 24 shows the fracture surface of

three-point bending experiment specimens. At 0 H, it presents the brittle fracture, and damage mechanism is mainly matrix cracking. And after dip specimen in high temperature water environment, fracture of specimens has more fiber pull out, less adhesive resin, the failure mechanism of materials into matrix cracking and interface debonding [22].

0 H   100 H   800 H

Fig. 23 Surface of three-point bending experiment specimen
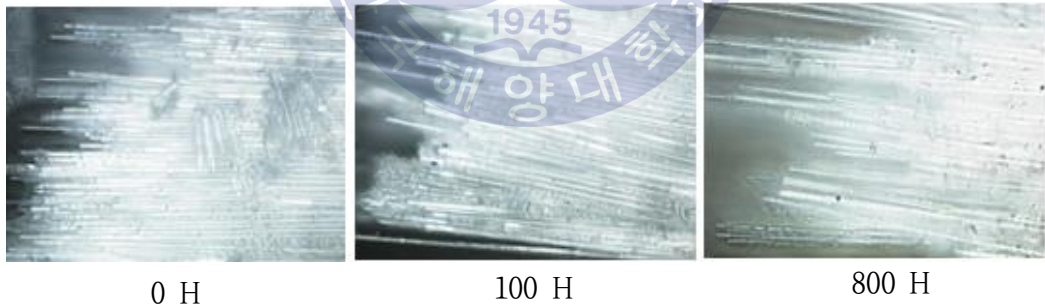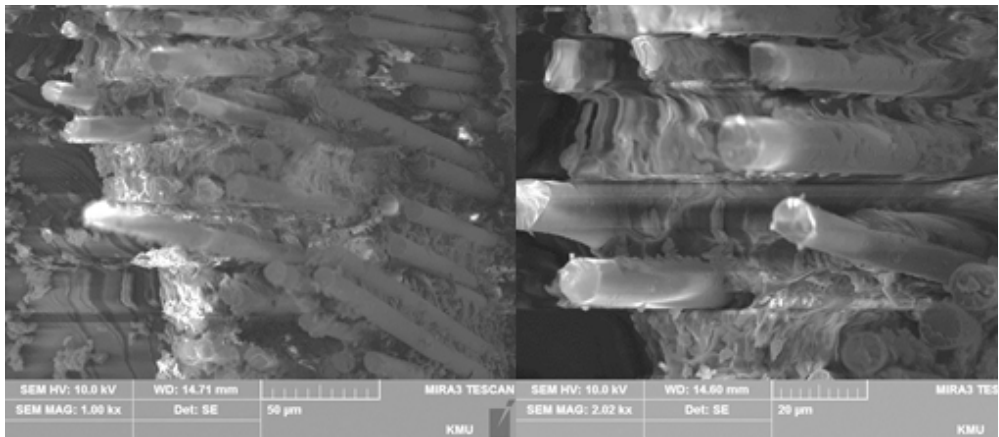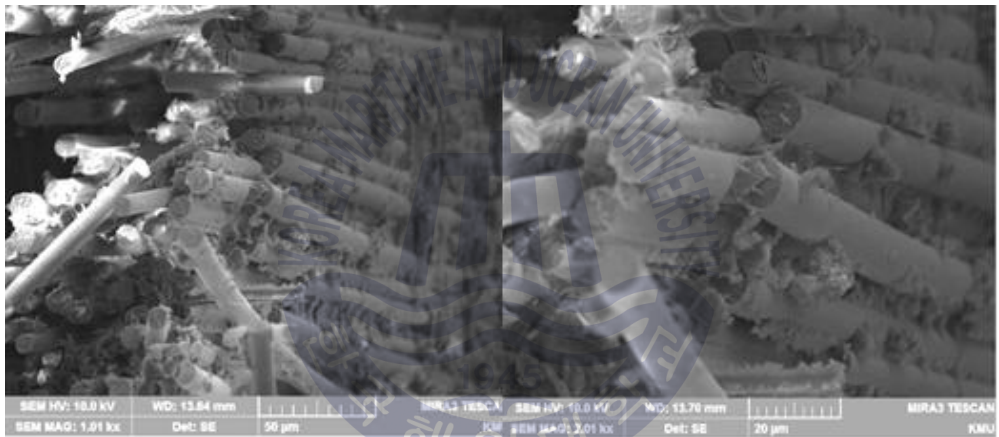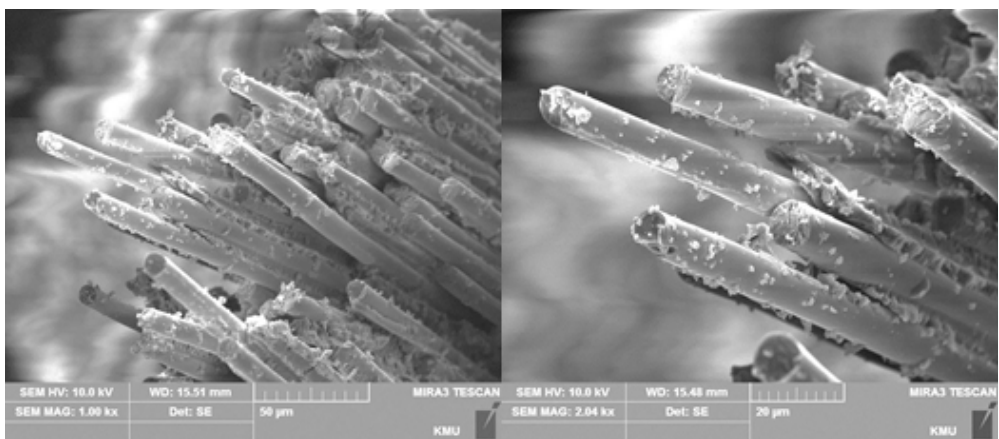

0 H   100 H   800 H

Fig. 24 Fracture surface of three-point bending experiment specimen

0 H

100 H

800 H

Fig. 25 Specimens fracture surface

Fig. 25 from top to bottom successively shows the specimen fracture after the three-point bending experiment without submerged in hot water (0 H) and submerged in hot water 100 hours (100 H) and 800 hours (800 H) at a temperature of 80℃. And the photos on the left side are magnified 1000 times, and 2000 times magnified on the right side. The resin is becoming less around the fiber with the increases with time can be observed clearly by using SEM. And the gaps between the fiber is becoming bigger, thus the mechanical properties decreased obviously.

Chapter 5 Conclusion

Experiments show that water absorption is almost no influence for the glass fiber reinforced polyester composites under different bending stress, and in 1000 H the moisture absorption rate is symmetrically, the maximum water absorption of test specimen is approximately 2.077%, and the diffusion coefficient is 0.001917.

The modulus of elasticity in bending is decreased firstly, then it is increased with the increasing immersion time, finally it has a downward trend. It recovers fast when the pressure is low, and recovers slow when the pressure is high.

Residual bending strength of the material in high temperature water environments show a deterioration trend with pressure increase. Bending strength degradation obey an exponential decay. Within 100H, the bending strength decline rate is proportional to the pressure.

By the calculation of material failure time under different pressures, ST life curve is shown, and uses a normalized model fatigue, stress corrosion cracking normalized intensity attenuation model is derived.

Fracture energy is similar to the residual bending strength, the degree of attenuation obey an exponential decay.

Acknowledgement

I would like to thank my parents for 26 years' breeding, love and support, as well as my elder sister's help and support. I would not have the chance to come here without them. I also would like thank my advising professor, Yun-Hae Kim, for his guidance and help in past two years. he is affable and approachable, and I learnt a lot from his profound knowledge and the lab's free learning environment, it will be my lifelong benefit. Last, I would like to thank doctor Jin-Cheol Ha and president Hee-Soo Yoon for dongdo basalt company for helping me on my korean life, and the members of the lab and school, I was very happy in their company. And they are my biggest wealth all my life.
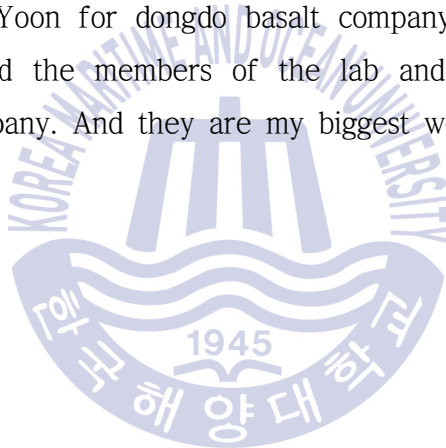
References

[1] Information on http://en.wikipedia.org/wiki/Glass_fiber

[2] Huang gu, 2009. Behaviours of glass fibre/unsaturated polyester composites under seawater environment, Materials and Design, pp. 1337–1340.

[3] A. Nakai & S. Ikegaki, 2000. Degradation of braided composites in hot water, Composites Science and Technology, pp. 325–331.

[4] Dong linlin, 2007. 玻璃纤维不饱和聚酯复合材料的海水老化研究,天津工业大学, pp. 6.

[5] Lv xiaojun & Zhang qi & Ma zhaoqing, 2005, Study of Hydrothermal Aging Effect on Mechanical Properties of Carbon Fiber / Epoxy Resin Composites, 材料工程, pp.50-53.

[6] A.Nakai,S. Ikegaki & H. Hamada, 2000, Degradation of braided composites in hot wate, Composites Science and Technology, pp. 325-331.

[7] Sun Bo & Li Yan, 2013, 复合材料湿热老化行为研究及其耐久性预测, 玻璃钢/ 复合材料, pp. 28-34.

[8] Zheng peng, 2011. VARTM工艺浸润过程及其应用基础研究, 中北大学, pp. 1-5.

[9] Ren ningbo, 2013. Characteristics of bending stress corrosion cracking of basalt fiber reinforced composite materials by different

fabrication methods, Korea maritime and ocean university, pp. 12.

[10] ASTM International, 2010. Standard Test Methods for Flexural Properties of Unreinforced and Reinforced Plastics and Electrical Insulating Materials (Designation: D790–10), pp. 4-6.

[11] A. Kootsookos & A.P. Mouritz, 2004. Seawater durability of glass- and carbon-polymer composites, Composites Science and Technology, pp. 1503–1511

[12] Zhou meng, 2013. GFRP与BFRP复合材料的湿热耐久性能研究, 哈尔滨工业大学, pp. 9.

[13] Sun hongxia, 2005. 复合材料湿环境下的性能研究, 天津工业大学, pp. 21-22.

[14] Information on http://en.wikipedia.org/wiki/Fick's_laws_of_diffusion

[15] Zhao peng, 2009. 纤维增强树脂基复合材料湿热老化性能研究,南京航空航天大学, pp. 10-29.

[16] 中国航空研究院编著, 2001. 复合材料结构设计手册, 航空工业出版社, pp. 477-480.

[17] Mahmood M. Shokrieh & Mahdi Memar, 2010. Stress Corrosion Cracking of Basalt/Epoxy Composites under Bending stress, Appl Compos Mater, pp. 121–135.

[18] Qiao Pizhong & Xu Yingwu, 2008. Mode-I fracture and durability of FRP-concrete bonded interfaces, Water Science and Engineering, pp. 47-60.

[19] Bryan Harris, 2003. Fatigue in composites, CRC Press, pp. 70-76.

[20] Zhao yanhu, 2002. 混凝土断裂过程中的能量分析研究,大连理工大学, pp. 16—17.

[21] Gao danying & zhang Tingyi, 2007. 三点弯曲下的钢纤维高强混凝土断裂能,水利学报, pp. 1116.

[22] Nan tiantian, 2013, Influence of bending load on the properties of CFRP under hygrothermal environment, 哈尔滨工业大学, pp. 30-36.